Tribhuvan University Journal
Vol. 36, No. 1: 1-17, June, 2021
Research Directorate, Tribhuvan University,
Kathmandu, Nepal
DOI: https://doi.org/10.3126/tuj.v36i01.43509

EVALUATION OF CORROSION CONDITION OF SOME STEEL-REINFORCED CONCRETE INFRASTRUCTURES AVAILABLE IN POKHARA VALLEY OF NEPAL

***Ishwor Laudari*[1], *Nav Raj Phulara*[2], *Madhab Gautam*[3], *Jagadeesh Bhattarai*[1*]**

[1]*Central Department of Chemistry, Kirtipur, TU.*
[2]*Teaching Assistant, Tri-Chandra M. Campus, Kathmandu, TU.*
[3]*Lecturer, Tribhuvan M. Campus, Tansen, TU.*
[3]*Professor, Central Department of Chemistry, Kirtipur, TU.*
**Corresponding author: bhattarai_05@yahoo.com*

ABSTRACT

Assessment of the corrosion condition of different types of eighty steel-reinforced concrete (SRC) structures of Pokhara Valley (Nepal) was carried out in the present study using a half-cell potential measurement (HCPM) method without destruction of specimens. It is concluded from the experimental results that the SRC structures found at dried places in Pokhara areas showed a low percentage (i.e., < 10%) of corrosion risk, while the fencing pillars used for decoration as well as boundary purposes, and the sewer pipes at damp places found under the high percentage (i.e., > 90%) of corrosion risk. The SRC infrastructures, which have rough, and cracked surfaces with high humid surrounding environments, are at high risk of corrosion. The SRC columns of the buildings in Pokhara Valley are at a slightly higher corrosion risk than the SRC roof structures.

Keywords: concrete infrastructure - corrosion assessment - half-cell corrosion potential - reinforced steel - voltmeter.

INTRODUCTION

An extensively used material in the construction section is concrete, which estimates more than 25 gigatonnes (per year) consumed globally (Green *et al.* 2020). It has high compression strength while its tensile strength and elasticity are poor (Angst 2018) and for this reason, usually

different carbon steels and stainless steels have been embedded in concrete structures to retain its enough tensile, shear, and even more compressive strengths combined with durability (Bhattarai 2010). The highly alkaline nature of cement paste with about 12 to 14 pH values (Revie & Uhlig 2008) provides high durability for several decades to the steel-reinforced structures with excellent corrosion protection when the structures are suitably designed, constructed, and preserved. However, research works on corrosion of different infrastructures of Nepal in the fields of soil corrosion (Bhandari *et al.* 2013, Dahal *et al.* 2021, 2018; Dhakal *et al.* 2014, Poudel *et al.* 2020, Regmi *et al.* 2015), corrosion inhibitors extracted from Nepal origin green plants (Katuwal *et al.* 2020, Subedi *et al.* 2019, Rana *et al.* 2017) and aqueous corrosion (Bhattarai 2021, 2020) so on are reported in literatures.

Nepal belongs to active seismic regions (Subedi & Chhetri 2019). The reinforcing concrete infrastructures and buildings mostly constructed without considering the corrosion damage problems, including seismic design principles before the April-2015 Gorkha earthquake (Sae-Long *et al.* 2019). Also, still practices against compliance with building standards (NBC-105 2020). It reported that the columns and beams are sensitive parts that can induce the entire infrastructures and buildings to collapse during earthquakes. Hence, the new model proposes to resolve such drawbacks of existing ones (Lee & Han 2021).

Researchers, structural engineers, and technologists needed to look over and recognize the problems of such unexpected corrosion damages of various SRC structures, particularly in urban areas and cities like Kathmandu Valley, its surrounding cities of Bagamati province, and also in Pokhara Valley of Gandaki province. For the sake of such undesirable corrosion damages of the reinforcing concrete structures, the first step is to estimate the corrosion condition of such SRC infrastructures. Considering the facts, a previous study focused on ascertaining the corrosion damage conditions of the SRC structure of the Kathmandu valley from the recorded open-circuit corrosion potential (OCCP) values and reported that such technique proved to be promising for predicting accurate information about different corrosion states of the SRC infrastructures (Phulara & Bhattarai 2019). Their study had successfully drawn the conclusion that > 90% corrosion

damages of the SRC infrastructures of Kathmandu Valley observed, mostly due to their surface roughness with high pore density and cracks.

In this context, this work was aimed to investigate the reinforced steel corrosion in concrete infrastructures of Pokhara Valley, based on the recorded OCCP values using an HCPM method in accordance with ASTM C876-15 standard (2015) to identify the deterioration condition of the SRC structures available in the Pokhara areas of the Gandaki province of Nepal. The findings of the present works rendered a categorization of solution methods for corrosion protection, maintenance, and repair using the world widely practiced standard methods.

MATERIALS AND METHODS

Corrosion conditions of the eighty reinforcing concrete infrastructures from the surroundings of the Pokhara Valley (Figure 1) were studied by recording their open-circuit corrosion potential (OCCP) or corrosion potential (ϕ_{corr}) using the HCPM method, as described in the ASTM standard (ASTM C876-15 2015) after visual examination of the sampling locations. All the analyzed SRC structures used for the present study were selected randomly and classified into building roof (20 sites), supporting building column (20 sites), sewer pipe (20 sites), dam-bridge (10 sites), and fencing pillar (10 sites).

Before the recording of the OCCP value of these reinforcing concrete structures, the details about their location conditions, types, physical, morphological properties were noted. Then, the ϕ_{corr} value of each reinforcing concrete structure at the randomly fixed four points named as 1, 2, 3, 4, was recorded using a Hong Kong made UNI-T model digital voltmeter against the saturated calomel electrode (SCE), and recorded ϕ_{corr} value is the average of four points. The SCE (reference) and the reinforced steel rod (working electrode) were connected to the voltmeter for recording potential values using the HCPM method, as described elsewhere (Bhattarai *et al.* 2021). It is meaningful to note that, all the ϕ_{corr} are expressed in SCE scale hereafter.

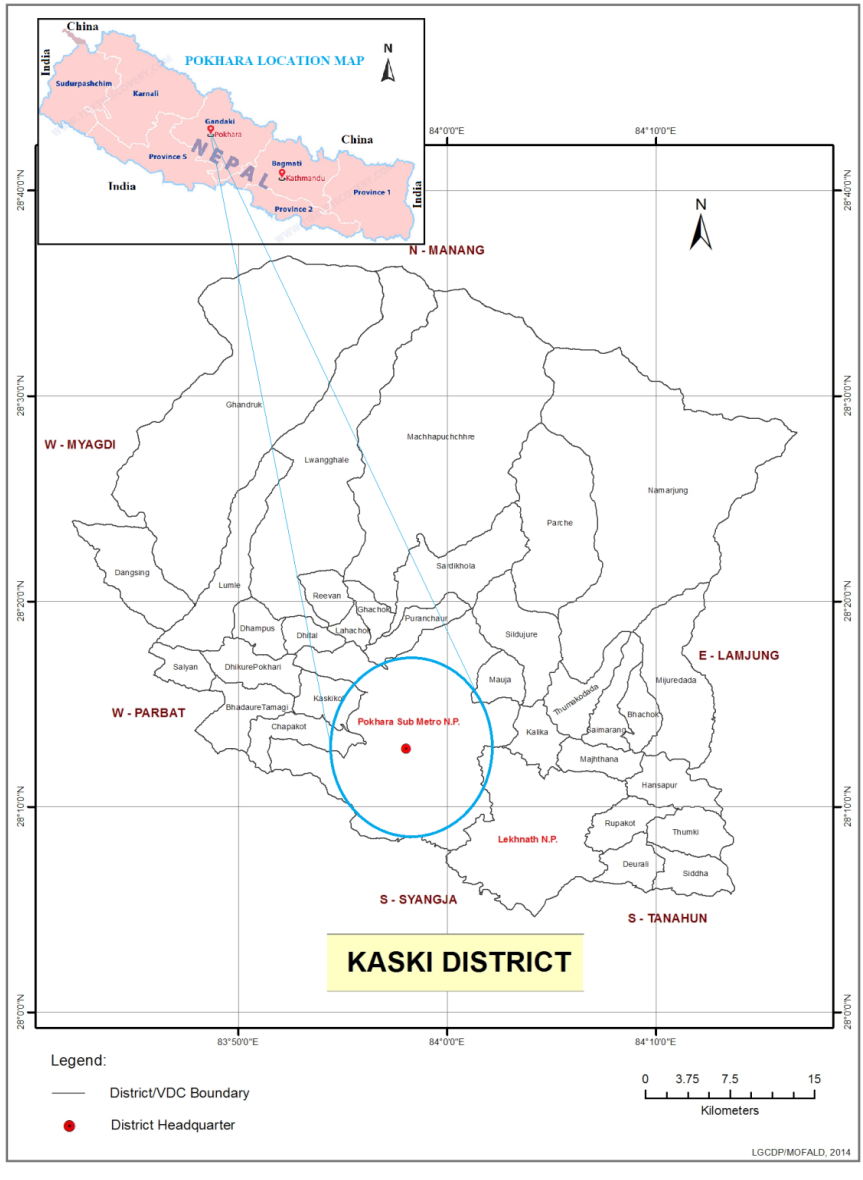

Figure 1: Location map of sampling sites at Pokhara Valley, Nepal

In the HCPM technique, the corrosion conditions of the SRC infrastructures are ascertained with the noted potentials in line with the ASTM C876-15 standard (2015). In this standard, the corrosion conditions of the steel rebar ascertain with the recorded ϕ_{corr} data, which is proving to be one of the reliable, easiest and cost-effective techniques to know the

corrosion conditions of the SRC infrastructures (Flores-Nicolas *et al.* 2021). The corrosion degree of steel considered to be low (i.e., < 10% corrosion) at the time of study when the average ϕ_{corr} is in the noble direction than −126 mV. Likewise, other two corrosion conditions of the SRC assume to be an uncertain (i.e., about 50% corrosion), and an extremely high corrosion risk (i.e., > 90%) was ascertained, as summarized in Table 1 (ASTM C876-15, 2015).

Table 1: ϕ_{corr} value and corrosivity of the SRC structures (ASTM C876-15, 2015)

ϕ_{corr} **(mV vs SCE)**	**Corrosion level of the SRC infrastructure**
< −276	High corrosion (HiC); i.e., > 90% corrosion risk
−276 to −126	Mid corrosion (MiC); i.e., about 50% corrosion risk or uncertain
> −126	Less corrosion (LeC); i.e., < 10% corrosion risk

RESULTS AND DISCUSSION

First of all, altogether 80 SRC infrastructure specimens, which grouped into building roof and supporting column, sewer pipe, dam-bridge, and fencing pillar were randomly picked out from the surroundings of Pokhara Valley of Nepal to study present work. Then, their physico-morphological properties (for examples, age, surface morphology and changes, the condition of the state) were noted before recording their ϕ_{corr} values, as given full procedure above in the experimental section. Also, photographs of these SRC specimens were taken which are not shown herein. The results of the physical and morphological properties of these 80 SRC specimens, including their mean ϕ_{corr} of four points as well as the standard deviation values of the building roofs, supporting columns, sewer pipes, and dam-bridge-fencing pillars are tabulated in Tables 2, 3, 4, and 5, respectively, in appendix section. The tables showed that corrosion conditions of that point or area at the time of ϕ_{corr} recorded of the reinforced steel in concrete specimens do not rely upon the age of the structures. It does not matter whether the concrete infrastructures are new or old, for depicting high, mid, and less corrosion degrees based on the ϕ_{corr} values.

The corrosion level of the reinforced steel in the concrete infrastructures depends mostly on morphological changes and destruction and surrounding environmental conditions of the sampled specimens. For the most analyzed SRC structures, wetness and destructed or spalling out

surfaces stated for consideration of either mid corrosion (i.e., the probability of uncertain corrosion) or high corrosion (i.e., the probability of more than 90% corrosion damage) level, as summarized the corrosion conditions in remark columns of Tables 2-5, based on the ASTM C876-15 standard (2015).

More details about the qualitative assessments of these three corrosion levels of the SRC infrastructures were ascertained from the recorded ϕ_{corr} for each sampled specimen of all categories of infrastructures, as depicted in Figure 2. Twenty SRC roofs of twenty buildings from different localities of the Pokhara Valley were randomly chosen to study their condition using the HCP method. Four points of each concrete roof specimen were monitored for their ϕ_{corr} values using a voltmeter, and the ϕ_{corr} values of the four attempts for all twenty specimens [Figure 2(a)], and the mean and standard deviation values are summarized in Table 2.

The ϕ_{corr} values were observed between −23 and −230 mV vs SCE, which are belonging to only two corrosion groups (i.e., LeC and MiC), not of HiC corrosion group based on the ASTM C876-15 standard (2015) which is presented diagrammatically, as depicted in Figure 3(a). Among twenty SRC roofs of the building, 55% (11 sample specimens) are considered to be LoC (i.e., a probability of less than 10 % corrosion occurs), while the remaining 45% (9 specimens) roofs are considered to be MiC with the mean ϕ_{corr} values within −128 and −224 mV, as shown in Figure 3(a) and also in Table 2. Furthermore, the ϕ_{corr} values of four points of each twenty concrete roof specimens are within the standard deviation potential value of less than 10 mV. The results pointed out that the measured ϕ_{corr} values of four points of a single sample specimen represent the real and more precise corrosion conditions of the SRC roof of all twenty buildings of the study areas. Also, such homogeneous ϕ_{corr} values of all four measurement points within the wide areas of the concrete infrastructure do not demonstrate the occurrence of localized types of corrosion, for example, the pitting, inter-granular or galvanic corrosion so on (Ebell *et al.* 2018).

Likewise, the almost same type of corrosion conditions, (i) the probability of less than 10 % corrosion damage (LeC), and (ii) uncertain to assign the corrosion condition either LeC or HiC with the recorded ϕ_{corr} values between −126 mV and −276 mV, are expected from the mean ϕ_{corr} values of all twenty old and newly constructed SRC building columns of the Pokhara Valley, as shown in Figure 2(b). It is found that about 40% of

Table 2: Physico-morphological description with mean ϕ_{corr}, standard deviation (n=4), and corrosion level of the SRC building roof specimens of the Pokhara Valley

Steel-reinforced Concrete Building Roof (BRf)				
Sample No.	**Physico-morphological properties of the specimens**	**ϕ_{corr} (mV vs SCE)**		
		Mean	**SD**	**Remark**
BRf-1	Old; smooth without cracking & spalling surface; damp, rust tints	-155	±3.34	MiC
BRf-2	New; smooth without cracking & spalling surface; dried, no tints	-69.5	±1.66	LeC
BRf-3	New; smooth without cracking & spalling surface; dried, no tints	-66.5	±2.29	LeC
BRf-4	New; porous without cracking & spalling surface; damp; no tints	-75.3	±3.56	LeC
BRf-5	Old; smooth without cracking & spalling surface; damp; rust tints	-224	±3.90	MiC
BRf-6	New; smooth without cracking & spalling surface; dried; no tints	-79.0	±3.16	LeC
BRf-7	Old; smooth without cracking & spalling surface; damp ; rust tints	-160	±3.91	MiC
BRf-8	New; smooth without cracking & spalling surface; dried; no tints	-72.2	±3.70	LeC
BRf-9	New; smooth without cracking & spalling surface; dried; no tints	-148	±3.56	MiC
BRf-10	Old; rough without cracking & spalling surface; damp; no tints	-38.3	±2.95	LeC
BRf-11	New; rough surface; cracking & spalling; dump; no tints	-178	±8.41	MiC
BRf-12	New; rough without cracking & spalling surface; damp; no tints	-181	±6.42	MiC
BRf-13	New; rough without cracking & spalling surface; damp; no tints	-52.8	±1.92	LeC
BRf-14	Old; rough without cracking & spalling surface; damp; no tints	-45.0	±4.74	LeC
BRf-15	New; smooth without cracking & spalling surface; dried; no tints	-120	±5.12	LeC
BRf-16	Old; smooth without cracking & spalling surface; damp; rust tints	-128	±3.42	MiC
BRf-17	New; smooth without cracking & spalling surface; dried; no tints	-25.0	±1.87	LeC
BRf-18	Old; rough & destructed surface; damp; rust tints	-134	±2.69	MiC
BRf-19	New; smooth without cracking & spalling surface; dried; no tints	-151	±3.27	MiC
BRf-20	New; smooth without cracking & spalling surface; dried; no tints	-46.2	±4.82	LeC

SD= standard deviation; LeC= less corrosion (<10% corrosion damage) & MiC= mid corrosion (uncertain state)

Table 3: Physico-morphological description with mean ϕ_{corr}, standard deviation (n=4), and corrosion degree of the building supporting SRC column specimens of the Pokhara Valley

Building supporting Steel-reinforced Concrete Column (CoC)				
Sample No.	*Physico-morphological properties of the specimens*	ϕ_{corr} *(mV vs SCE)*		
		Mean	*SD*	*Remark*
CoC-1	Old; rough with cracking & spalling surface; dried; rust tints	-115	±6.87	LeC
CoC-2	Old; smooth with few cracking & spalling surface; dried; rust tints	-128	±5.07	MiC
CoC-3	New; smooth without cracking & spalling; damp; rust tints	-128	±2.50	MiC
CoC-4	New; smooth without cracking & spalling surface; dried; no tints	-94.3	±7.01	LeC
CoC-5	New; smooth without cracking & spalling; damp; rust tints	-132	±3.96	MiC
CoC-6	Old; rough with cracking & spalling surface; dried; rust tints	-114	±4.66	LeC
CoC-7	Old; rough with cracking & spalling surface; dried: rust tints	-195	±3.03	MiC
CoC-8	Old; rough without cracking & spalling surface; damp; rust tints	-225	±6.87	MiC
CoC-9	New; smooth without cracking & spalling; damp; rust tints	-79.7	±4.92	LeC
CoC-10	Old; rough with cracking & spalling surface; damp; rust tints	-245	±3.03	MiC
CoC-11	Old; rough with cracking & spalling surface; dried; rust tints	-140	±5.36	MiC
CoC-12	New; smooth without cracking & spalling; dried; no tints	-114	±4.58	LeC
CoC-13	Old; rough with cracking & spalling surface; damp; rust tints	-245	±4.60	MiC
CoC-14	Old; rough without cracking & spalling surface; damp; rust tints	-127	±3.70	MiC
CoC-15	Old; rough with cracking & spalling surface; dried; rust tints	-130	±6.18	MiC
CoC-16	New; smooth without cracking & spalling; dried; no tints	-126	±5.68	MiC
CoC-17	Old; rough with cracking & spalling surface; dried; no tints	-137	±2.92	MiC
CoC-18	Old; rough with cracking & spalling surface; dried; rust tints	-123	±1.92	LeC
CoC-19	New; smooth without cracking & spalling; dried; no tints	-92.8	±3.34	LeC
CoC-20	New; smooth without cracking & spalling; dried; no tints	-101	±6.57	LeC

SD= standard deviation; LeC= less corrosion (<10% corrosion damage); MiC= mid corrosion (uncertain state)

Table 4: Physico-morphological description with mean ϕ_{corr}, standard deviation (n=4), and corrosion condition of the SRC sewer pipes used in Pokhara Valley

Steel-reinforced Concrete Sewer Pipe (SwP)				
Sample No.	*Physico-morphological properties of the specimens*	ϕ_{corr} *(mV vs SCE)*		
		Mean	*SD*	*Remark*
SwP-1	New; smooth without cracking & spalling surface; dried; no tints	-72.0	±1.87	LeC
SwP-2	Old; smooth without cracking & spalling surface; moist; no tints	-48.0	±2.24	LeC
SwP-3	Old; rough surface; cracking & spalling; moist; rust tints	-366	±2.86	HiC
SwP-4	New; smooth without cracking & spalling surface; dried; no tints	-55.8	±2.59	LeC
SwP-5	New; rough surface; no cracking & spalling; moist; rust tints	-343	±3.08	HiC
SwP-6	Old; smooth without cracking & spalling surface; moist; no tints	-44.7	±4.38	LeC
SwP-7	Old; rough surface; no cracking & spalling; moist; rust tints	-335	±1.92	HiC
SwP-8	New; smooth surface; cracking & spalling; dried; rust tints	-346	±1.22	HiC
SwP-9	New; smooth without cracking & spalling surface; dried; no tints	-164	±2.06	MiC
SwP-10	Old; smooth surface; cracking & spalling; damp; rust tints	-355	±1.48	HiC
SwP-11	Old; smooth surface; cracking & spalling; damp; rust tints	-259	±4.74	MiC
SwP-12	New; smooth without cracking & spalling surface; dried; no tints	-92.0	±4.42	LeC
SwP-13	New; smooth surface; no cracking & spalling; damp; no tints	-73.5	±5.85	LeC
SwP-14	New; rough surface; no cracking & spalling; damp; rust tints	-336	±2.17	HiC
SwP-15	Old; smooth without cracking & spalling surface; damp; rust tints	-130	±1.92	MiC
SwP-16	New; smooth surface; cracking & spalling; dried; rust tints	-329	±2.06	HiC
SwP-17	New; smooth without cracking & spalling surface; dried; no tints	-233	±3.49	MiC
SwP-18	New; smooth without cracking & spalling surface; dried; no tints	-136	±1.79	MiC
SwP-19	Old; rough surface; no cracking & spalling; danp; rust tints	-345	±1.58	HiC
SwP-20	Old; smooth without cracking & spalling surface; dried; rust tints	-134	±3.16	MiC

SD= standard deviation; LeC= less corrosion (<10% corroded); MiC= mid corrosion (uncertain state); HiC= high corrosion (>90% corroded)

Table 5: Physico-morphological description with mean ϕ_{corr}, standard deviation (n=4), and corrosion condition of the SRC dam-bridge and fencing pillar available in Pokhara Valley

Steel-reinforced Dam - Bridge (BmB) and Fencing Pillar (FnP)				
Sample No.	*Physico-morphological properties of the specimens*	ϕ_{corr} *(mV vs SCE)*		
		Mean	*SD*	*Remark*
DaB-1	Old; smooth without cracking & spalling surface; damp; no tints	-260	±9.54	MiC
DaB-2	New; smooth without cracking & spalling surface; damp; no tints	-21.0	±5.61	LeC
DaB-3	New; smooth surface; cracking & spalling; damp; rust tints	-263	±4.30	MiC
DaB-4	Old; smooth without cracking & spalling surface; damp; no tints	-192	±5.15	MiC
DaB-5	New; smooth without cracking & spalling; damp; rust tints	-157	±8.41	MiC
DaB-6	New; smooth without cracking & spalling; damp; rust tints	-126	±3.96	MiC
DaB-7	Old; smooth with cracking & spalling surface; dried; rust tints	-276	±2.86	HiC
DaB-8	New; smooth without cracking & spalling; damp; rust tints	-119	±6.83	MiC
DaB-9	Old; smooth without cracking & spalling; dried; no tints	-127	±4.02	MiC
DaB-10	New; smooth without cracking & spalling; damp; rust tints	-129	±3.70	MiC
FnC-11	Old; rough & delaminated surface; dap; rust tints	-294	±2.59	HiC
FnC-12	Old; rough & destructed surface; damp; rust tints	-276	±3.32	HiC
FnC-13	Old; rough with cracking & spalling surface; dried; rust tints	-290	±4.97	HiC
FnC-14	Old; rough with cracking & spalling surface; dried; rust tints	-295	±4.30	HiC
FnC-15	Old; rough with cracking & spalling surface; damp; rust tints	-281	±3.20	HiC
FnC-16	Old; rough & destructed surface; damp; rust tints	-314	±4.66	HiC
FnC-17	Old; rough & destructed surface; damp; rust tints	-295	±3.03	HiC
FnC-18	Old; rough with cracking & spalling surface; damp; rust tints	-325	±6.87	HiC
FnC-19	Old; rough with cracking & spalling surface; damp; rust tints	-214	±1.80	MiC
FnC-20	Old; smooth with cracking & spalling surface; damp; rust tints	-245	±3.03	MiC

SD= standard deviation; LoC= less corrosion (<10% corroded); MiC= mid corrosion (uncertain state); HiC= high corrosion (>90% corroded)

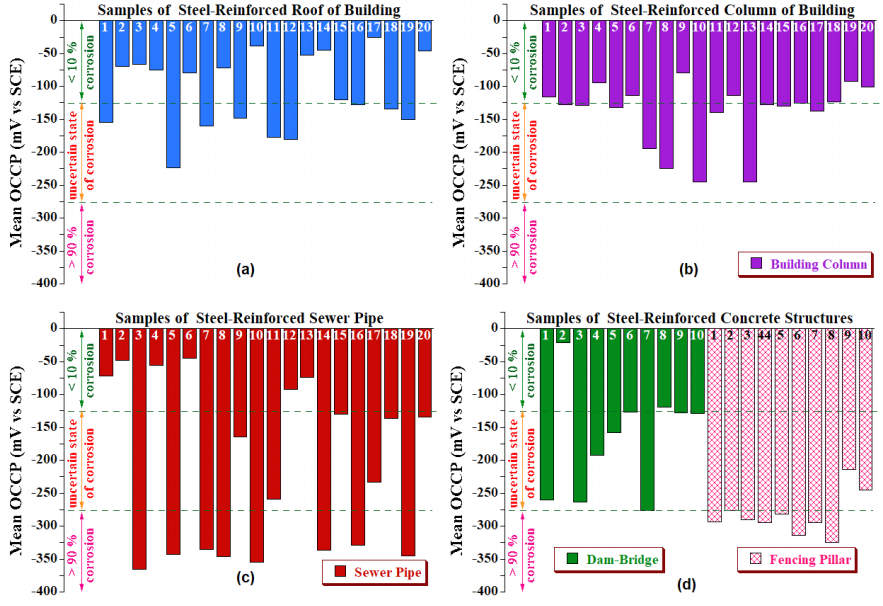

Figure 2: Mean ϕ_{corr} values showing three corrosion conditions of the SRC infrastructures of (a) building roof, (a) building column, (c) sewer pipe, and (d) dam-bridge and fencing pillar

the building columns (i.e., 8 sample specimens) have less than 10% chance of the corrosion risk (LeC) having the average ϕ_{corr} value more positive values than −126 mV, while the remaining 60% (12 sample specimens) building columns with the average ϕ_{corr} values between −126 mV and −245 mV are considered as the corrosion condition at uncertain based on the classification of the ASTM C876-15 standard (2015), which is plainly shown in Figure 3.

In general, columns of the older SRC buildings should have more corrosion-prone and fragile than new ones and hence easily collapsed the entire structures during natural disasters (e.g., earthquake). However, from the present findings, it can be said that the vertical columns of the building are found to be more vulnerable than the reinforced concrete roof of the building alike as reported in literatures (Lee & Han 2018), mostly due to the micro-cracking, disbanded, spalling, and crushing, at steel-concrete interfaces (Yue *et al.* 2016). Early researches revealed the reinforced concrete columns constructed before the 1970s exhibited poor corrosion-resistance behavior (Galanis & Moehle 2015). In a recent study, a numerical

model has been proposed to prevent from such corrosion problems (Lee & Han, 2021).

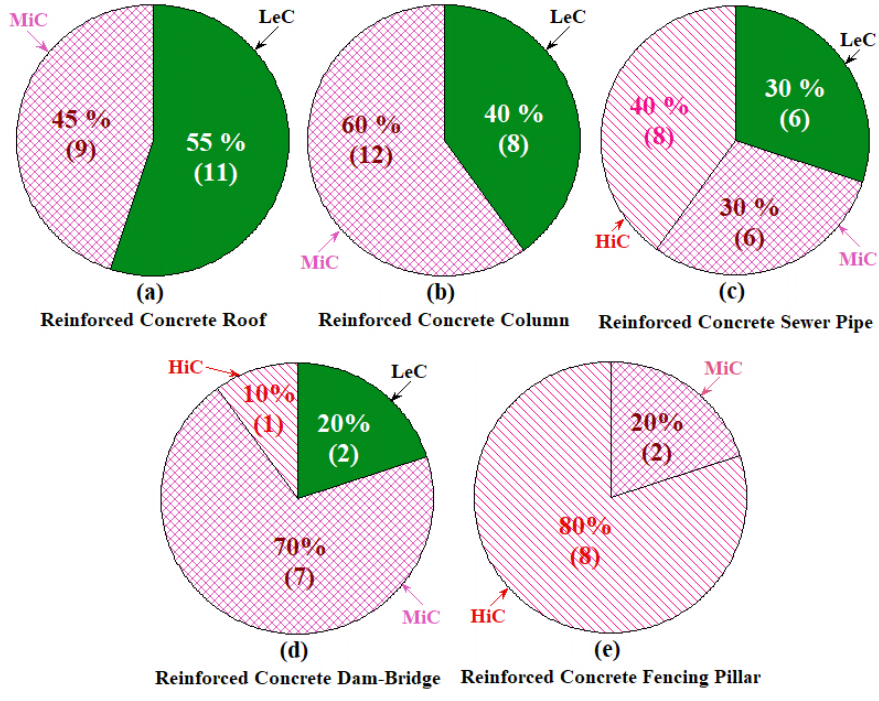

Figure 3: Pie charts showing three corrosion conditions of the SRC infrastructures of (a) building roof, (a) building column, (c) sewer pipe, and (d) dam-bridge and fencing pillar

On the Other hand, among 20 sampled SRC sewer pipes used in different localities of the Pokhara Valley, nearly 30% (6 samples) were in good condition showing less than 10% chance of the corrosion risk with showing the mean ϕ_{corr} value in noble than −126 mV, as depicted in Figures 2(c) and 3(c), and also summarized the data in Table 4. Also, the figure distinctly showed that six sewer pipes (i.e., 30%) were to be in the mild corrosion condition with the average ϕ_{corr} values in the range of −126 mV to −276 mV, while remaining 40% of pipes (4 samples) could be categorized as high corrosion condition, i.e., showing more than 90% probability of the corrosion damage having the average ϕ_{corr} value in less noble than −276 mV.

Figure 2(d) shows the average ϕ_{corr} values of 10 sampling sites of dam-bridge and 10 samples of fencing pillar used around the Pokhara Valley which are present in Table 5 also. All the recorded ϕ_{corr} values of these ten dam-bridge concrete infrastructures are in between –21 mV to –119 mV, and only two (10%) dam-bridges are considered as LeC expecting < 10% corrosion damage risk, while only one (10%) dam-bridge of Pokhara Valley could be grouped to the highly corroded level (HiC) with > 90% corrosion damage, as shown in Figure 3(d). The rest of seven (70%) samples among the ten dam-bridge samples could be considered as the uncertain corroded state based on the ASTM C876-15 standard (2015). These results revealed that most of the dam-bridges of Pokhara Valley are high prone state due to corrosion damages. Moreover, the ϕ_{corr} values of 10 fencing pillars were recorded between –214 mV and –325 mV, as tabulated in Table 5.

The resultant ϕ_{corr} values of all samples of fencing pillars are shown in Figures 2(d) and 3(e) which indicated that 80% of samples among the ten fencing pillars have > 90% corrosion risk of the SRC, while the remaining two pillars; FcP-9 and FcP-10 [Fig. 3(e)] specimens are considered to be mildly corroded with the average ϕ_{corr} values of −214 mV and −245 mV, respectively, as depicted in Figure 2(d) and Table 5 also. These results indicated that most of the entire fencing pillars do not function for a long time without the repairs.

CONCLUSIONS

The corrosion condition of 80 reinforced steel in different five categories of the concrete infrastructures of the Pokhara Valley (Nepal) was investigated using the HCPM method following the ASTM Standards. The results indicate that fencing pillars, old sewer pipes, and dam bridges are at high corrosion risk in moist conditions. Besides, the SRC infrastructures with porous/rough surfaces are at high corrosion risk. Present research concluded that the HCPM provides precious information on the likelihood of corrosion, and helps for the quality assurance of the SRC repair and rehabilitation. Depending on the measured ϕ_{corr} values, the probability of active corrosion damages of the SRC infrastructures even in large areas could be successfully assessed regularly in a short time without investigating huge amounts of money.

REFERENCES

Angst, U.M. (2018). Challenges and opportunities in corrosion of steel in concrete. *Materials and Structures*, **51**(4). https://doi.org/10.1617/s11527-017-1131-6

ASTM C876-15 (2015). *Standard test method for corrosion potentials of uncoated reinforcing steel in concrete*. ASTM International, West Conshohocken, PA, USA, p8. https://doi.org/10.1520/C0876-15

Bhandari, P.P., Dahal, K.P. & Bhattarai, J. (2013). The corrosivity of soil collected from Araniko Highway and Sanothimi areas of Bhaktapur. *Journal of Institute of Science and Technology*, **18**(1):71-77. https://www.researchgate.net/publication/311560647. Accessed: 19.04.2021.

Bhattarai, J. (2010). *Frontiers of corrosion science*. 1st edition, Kshitiz Publication, Kirtipur, Nepal, p304.

Bhattarai, J. (2020). Review on in-depth analysis of the passive films of W-xTi alloys by angle-resolved X-ray photoelectron spectroscopy. *Science Journal of Chemistry*, **8**(2):28-35. http://dx.doi.org/10.11648/j.sjc.20200802.12

Bhattarai, J. (2021). An overview on the non-destructive in-depth surface analysis of corrosion-resistant films: A case study of W-xCr deposits in 12 M HCl solution. *Bibechana*, **18**(1):201-213. https://doi.org/10.3126/bibechana.v18i1.29222

Bhattarai, J., Somai, M., Acharya, N., Giri, A., Roka, A. & Phulara, N.R (2021). Study on the effects of green-based plant extracts and water-proofers as anti-corrosion agents for steel-reinforced concrete slabs. *E3S Web of Conferences*, **302**, 02018. https://doi.org/10.1051/e3sconf/202130202018

Dahal, K.P., Karki, R.K. & Bhattarai, J. (2018). Evaluation of corrosivity of soil collected from the central part of Kathmandu Metropolis (Nepal) to water supply metallic pipes. *Asian Journal of Chemistry*, **30**(7):1525-1530. https://doi.org/10.14233/ajchem.2018.21211

Dahal, K.P., Timilsena, J.N., Gautam, M. & Bhattarai, J. (2021). Investigation on a probabilistic model for corrosion failure level of

buried pipelines in Kirtipur urban areas (Nepal). *Journal of Failure Analysis and Prevention*, **21**(1):914-926. https://doi.org/10.1007/s11668-021-01138-2

Dhakal, Y.P., Dahal, K.P. & Bhattarai, J. (2014). Investigation on the soil corrosivity towards the buried water supply pipelines in Kamerotar town planning areas of Bhaktapur, Nepal. *Bibechana*, **10**:82-91. http://dx.doi.org/10.3126/bibechana.v10i0.8454

Ebell, G., Burkert, A. & Mietz, J. (2018). Detection of reinforcement corrosion in reinforced concrete structures by potential mapping: Theory and practice. *International Journal of Corrosion*, **2018**, 3027825. https://doi.org/10.1155/2018/3027825

Flores-Nicolas, A., Flores-Nicolas, M. & Uruchurtu-Chavarin, J. (2021). Corrosion effect on reinforced concrete with the addition of graphite powder and its evaluation on physical-electrochemical properties. *Revista ALCONPAT*, **11**(1):18-33. https://doi.org/10.21041/ra.v11i1.501

Galanis, P.H. & Moehle, J.P. (2015). Development of collapse indicators for risk assessment of older-type reinforced concrete buildings. *Earthquake Spectra*, **31**(4):1991-2006. http://dx.doi.org/10.1193/080613EQS225M

Green, W., Collins, F. & Forsyth, M. (2020). Up to date overview of aspects of steel reinforcement corrosion in concrete. *In:* Brian Cherry (ed.) *Paper series*. The Australasian Corrosion Association Inc. https://membership.corrosion.com.au/blog/up-to-date-overview

Katuwal, P., Regmi, R., Joshi, S. & Bhattarai, J. (2020). Assessment on the effective green-based Nepal origin plants extract as corrosion inhibitor for mild Steel in bioethanol and its blend. *European Journal of Advanced Chemistry Research*, **1**(5):1-13. https://doi.org/10.24018/ejchem.2020.1.5.16

Lee, C.S. & Han, S.W. (2018). Computationally effective and accurate simulation of cyclic behavior of old reinforced concrete columns. *Engineering Structures*, **173**:892-907. https://doi.org/10.1016/j.engstruct.2018.07.020

Lee, C.S. & Han, S.W. (2021). An accurate numerical model simulating hysteretic behavior of reinforced concrete columns irrespective of types of loading protocols. *International Journal of Concrete Structures and Materials*, **15**:5. https://doi.org/10.1186/s40069-020-00446-5

NBC-105 (2020). Nepal national building code. *In:* MOUD (ed.) *Seismic design of buildings in Nepal*. Ministry of Urban Development, Government of Nepal, Kathmandu, p96. https://www.moud.gov.np/storage/listies/November2020/seismic-design-of-building-in-nepal.pdf. Accessed: 19.04.2021

Phulara, N.R. & Bhattarai, J. (2019). Assessment on corrosion damage of steel-reinforced concrete structures of Kathmandu valley using corrosion potential mapping method. *Journal of the Institute of Engineering*, **15**(2):47-56. https://doi.org/10.3126/jie.v15i2.27640

Poudel, A., Dahal, K.P. & Bhattarai, J. (2020). A classification approach for corrosion rating of soil to buried water pipelines: A case study in Budhanilkantha-Maharajganj roadway areas of Nepal. *World Journal of Applied Chemistry*, **5**(3):47-56. http://dx.doi.org/10.11648/j.wjac.20200503.12

Rana, M., Joshi, S. & Bhattarai, J. (2017). Extract of different plants of Nepalese origin as a green corrosion inhibitor for mild steel in 0.5 M NaCl solution. *Asian Journal of Chemistry*, **29**(5):1130-1134. https://doi.org/10.14233/ajchem.2017.20449

Regmi, S.K., Dahal, K.P. & Bhattarai, J. (2015). Soil corrosivity to the buried pipes used in Lalitpur, Kathmandu Valley, Nepal. *Nepal Journal of Environmental Science*, **3**(1):15-20. https://doi.org/10.3126/njes.v3i0.22730

Revie, R.W. & Uhlig, H.H. (2008). *Corrosion and corrosion control*: *An introduction to corrosion science and engineering*. 4th edition, John Wiley and Sons, Inc., Hoboken, New Jersey, USA, p490.

Sae-Long, W., Limkatanyu, S., Prachasaree, W., Horpibulsuk, S. & Panedpojaman, P. (2019). Nonlinear frame element with shear-flexure interaction for seismic analysis of non-ductile reinforced

concrete columns. *International Journal of Concrete Structure and Materials*, **13**:1-19. https://doi.org/10.1186/s40069-019-0343-2

Subedi, B.N., Amgain, K., Joshi, S. & Bhattarai, J. (2019). Green approach to corrosion inhibition effect of *Vitex negundo* leaf extract on aluminum and copper metals in biodiesel and its blend. *International Journal of Corrosion and Scale Inhibition*, **8**(3):744-759. http://dx.doi.org/10.17675/2305-6894-2019-8-3-21

Subedi, S. & Chhetri, M.B.P. (2019). Impacts of the 2015 Gorkha earthquake: Lessons learned from Nepal. *In:* Santos-Reyes, J. (ed.) *Earthquakes*. Chapter-5, IntechOpen, Rijeka, p16. https://doi.org/10.5772/intechopen.85322

Yue, J., Qian, J. & Beskos, D.E. (2016). A generalized multi-level seismic damage model for RC framed structures. *Soil Dynamics and Earthquake Engineering*, **80**:25-39. https://doi.org/10.1016/j.soildyn.2015.10.005